

Polyaniline Nanofibers for *In Situ* MAO-Catalyzed Polymerization of Ethylene

Nara Regina de Souza Basso,¹ Felipo Oliveira,¹ Ana Paula Graebin,¹ Cássio Stein Moura,¹ Fabiana de Carvalho Fim,² Griselda Barrera Galland,² Leila Bonnaud,³ Oltea Murariu,³ Philippe Dubois³

¹Faculdade de Química, Pontifícia Universidade Católica do Rio Grande do Sul-Brasil, Av. Ipiranga 6681, Porto Alegre 90619-900, Brazil

²Instituto de Química, Universidade Federal do Rio Grande do Sul, Av. Bento Gonçalves, 9500, Porto Alegre 91570-970, Brazil

³Laboratory of Polymeric and Composite Materials (LPCM), Center of Innovation and Research in Materials and Polymers (CIRMAP), University of Mons (UMONS) and Materia Nova Research Center, Place du Parc 23, B-7000 Mons, Belgium

Correspondence to: N. R. D. S. Basso (E-mail: nrbass@pucrs.br)

ABSTRACT: In this work electro-conductive polyaniline nanofibers (PAni-nanofibers) were prepared via interfacial methodology. Scanning electron microscopy (SEM) and transmission electron microscopy (TEM) observations revealed that the synthesized PAni-nanofibers present high aspect ratio with an average diameter of 80 nm, while they exhibit high conductivity (DC conductivity values: $4.19 \pm 0.21 \text{ S cm}^{-1}$). After specific treatment to remove moisture and remaining trapped HCl from PAni-nanofibers, it was possible to prepare promising polyethylene (PE)/PAni composites by *in situ* polymerization of ethylene using bis(cyclopentadienyl) zirconium(IV) dichloride (Cp_2ZrCl_2) and methylaluminoxane (MAO) as catalytic system. More precisely, various contents of PAni-nanofibers (from 0.2 to 7 wt %) were successfully incorporated in the *in situ* produced PE/PAni nanocomposites. PAni-nanofibers were found to affect significantly the crystallization of the polyolefinic matrix while preserving its thermal stability. Preliminary measurements of electric properties showed PAni-nanofibers are able to bring electro-conductive properties to the *in situ* polymerized PE/PAni composites. © 2014 Wiley Periodicals, Inc. *J. Appl. Polym. Sci.* **2014**, *131*, 41197.

KEYWORDS: composites; conducting polymers; fibers; nanostructured polymers; polyolefins

Received 24 March 2014; accepted 22 June 2014

DOI: 10.1002/app.41197

INTRODUCTION

Polyaniline (PAni) is a conjugated polymer that exhibits excellent electrical conductivities, thermal stability, and readily synthesized from a low-cost monomer. However, its reduced processability and poor mechanical properties limit its use as polymer matrix. Nevertheless, PAni can be used as particles that demonstrated a great potential as new conductive filler for polymers.¹ These composites can be easily processed in the melt and enlarge the possibilities for manufacturing new technical materials for applications such as antistatic packaging, electromagnetic shielding, anticorrosion shielding or semiconductors.

The conventional aniline polymerization is carried out in aqueous solution media in which aniline is dissolved in a strong acid solution at low temperature (0–5°C) and the polymerization is initiated when an oxidant is slowly added. Conventional polyaniline synthesis produces particles with irregular shapes. The basic morphological unit for chemically synthesized polyaniline appears to

be nanofibers with average diameters of 30–35 nm. When more oxidant is added, the nanofibers become scaffolds for secondary growth of polyaniline, which results in irregular shaped agglomerates containing nanofibers and mostly particulates.²

It has already been reported that polyaniline nanofibers (PAni-nanofibers) present several advantages in fabricating nanodevices and in preparing nanoscale electrical connections in highly conducting polymer composites, because of their high surface contact area.³ Therefore, different mechanisms and methodologies for synthesizing PAni-nanofibers have been investigated in the literature.⁴

The interfacial polymerization is quite convenient to prepare PAni-nanofibers. In this method, aniline is solubilized in an organic solvent, the oxidant in an aqueous acidic solution and the polymerization only occurs at the interface of the biphasic system where all reagents needed for the reaction are located.⁵ According to the mechanism that supports this methodology,

the nanofibers are formed when the secondary overgrowth, which results in irregular PANi particles, is hindered.^{2,5}

Composites with polyolefin matrix and PANi can be prepared by *in situ* oxidation polymerization of aniline in presence of the polymer matrix or dispersing PANi in a solution or in a melt of another polymer.⁶ Another possibility is *in situ* polymerization of olefins in presence of PANi. Although only few studies are reported in the literature for PANi, this method proved to have great potential as various studies have been successfully applied to other types of particles (organomodified clays, carbon nanotubes, graphene layers, and so forth) allowing for promoting more uniform dispersion of the nanofiller in the matrix.^{7,8} The *in situ* polymerization of olefins is even more attractive when metallocene catalysts are used because they have unique catalytic properties such as high activity and good control over the molecular weight and dispersity.⁹ However, it should be considered that the metallocene catalyst can be easily deactivated in presence of water traces or any other impurities present in the reaction medium, for example acidic species used as dopant in aniline polymerization.

It is known that PANi can absorb water molecules reversibly and irreversibly.¹⁰ Dry samples can absorb water by keeping PANi in humid ambient. The reversibly absorbed water can exist in two different forms. The first is weakly bonded to the polymer chain by hydrogen bonding, which can be removed from PANi with a flow of nitrogen or under dynamic vacuum. The second form has higher activation energy than the hydrogen bonding energy and it has been suggested that it results from the formation of chemical bonds with the PANi polymer backbone and it can be removed out by heating at the temperature range of 70–150°C.^{11,12} There also exists the irreversibly absorbed water that can only be removed out from polymer matrix at higher temperature range of 200–350°C. These strongly bounded water molecules act as a secondary dopant and it is often named as bounded water.^{11,12} Accordingly, for producing PE/PANi-nanofiber nanocomposites by *in situ* catalyzed polymerization it is necessary to completely remove both the reversibly absorbed water molecules from PANi chains and the excess of acid dopant molecules as they will be detrimental to the catalytic system readily deactivating it.

In this work PANi-nanofiber have been first synthesized by interfacial polymerization and then used for producing polyethylene-based composites by means of metallocene/methylaluminumoxane (MAO)-catalyzed *in situ* polymerization of ethylene. In order to avoid any deactivation of the MAO-based catalytic system, it has been necessary to adapt the PANi-nanofiber purification and drying processes allowing for preserving an efficient catalysis and polymerization step with good control over the morphology of the resulting nanocompositions.

EXPERIMENTAL

Materials

Aniline (Merck) of analytical grade was distilled before use. Ammonium peroxydisulfate, toluene (F. Maia) and hydrochloric acid (Merck) as analytical grade were used without any further purification. In the synthesis of PE/PANi nanocomposites all

manipulations were performed under inert atmosphere (nitrogen or argon) using standard Schlenk techniques. Toluene was dried over metallic sodium and benzophenone and distilled before use. MAO (Aldrich 10 wt % Al in toluene solution) and bis(cyclopentadienyl)zirconium dichloride (Cp₂ZrCl₂) (Sigma-Aldrich) were used as received.

Synthesis of PANi-Nanofibers

PANi-nanofibers were synthesized according to the interfacial polymerization method previously described in the literature.^{5,13} A 5.48 mmol amount of aniline was dissolved in 50 mL toluene. 1.26 mmol of ammonium peroxydisulfate (APS) and 0.5 mol of hydrochloric acid were dissolved in 50 mL water. The aniline organic solution was slowly added in the aqueous solution. The resulting two-phase system was left undisturbed for 18 h and after this period the aqueous solution was filtered and the dark green precipitate washed repeatedly with acetone to remove impurities. The resulting nanofibers were dried at room temperature for 48 h in a desiccator with silica gel as drying agent.

Preparation of PE/PANi Composites

To improve the removal of moisture and free dopant acid, the PANi-nanofibers were washed repeatedly with a solution of water and acetone until pH 4. Then the sample was dried under vacuum oven at 80°C for 30 h. Before the polymerization the recovered nanofibers were stirred with 20 wt % of MAO for 30 min in dried toluene.

The polymerization reactions were carried in a 100 mL PARR reactor. Toluene was used as solvent, MAO as cocatalyst (Al/Zr = 1000) and Cp₂ZrCl₂ as catalyst (2×10^{-6} mol). The reactions were performed at 60°C for 30 min using an ethylene pressure of 1.6 bars. The PANi-nanofibers previously treated with MAO were added to the reactor as filler at different given amounts.

Characterization of the PANi-Nanofiber and PE-Based Composites. The IR spectroscopy data of PANi-nanofibers were obtained on a Prestige 21 Shimadzu spectrometer using KBr. UV spectra were performed on a Cary 50 Bio Varian spectrometer using water as solvent.

Scanning electron microscopy (SEM) was performed with a Philips microscope, model XL30, operating at 20 kV. The samples were prepared by sample deposition in an aluminum stub and gold metalized. Transmission electron microscopy (TEM) images were obtained using a transmission electron microscope JEOL 1011 operated at 100 kV. All samples were prepared by deposition of a decaline solution drop on a grid of copper of 300 mesh covered with amorphous carbon.

The thermogravimetric analysis (TGA) was carried out using a Q5000IR TGA from TA Instruments. The experiment was performed under N₂ atmosphere from 25 to 400°C (PANi-nanofibers) and from 25 to 700°C (nanocomposites) at a heating rate of 10°C/min. The differential scanning calorimetric (DSC) study was carried out using a Q20 DSC from TA Instruments, under N₂ atmosphere from 20 to 160°C at the heating rate 10°C/min.

To evaluate the electrical properties of PANi-nanofibers, the collected polymeric powder was compressed in a cylindrical matrix

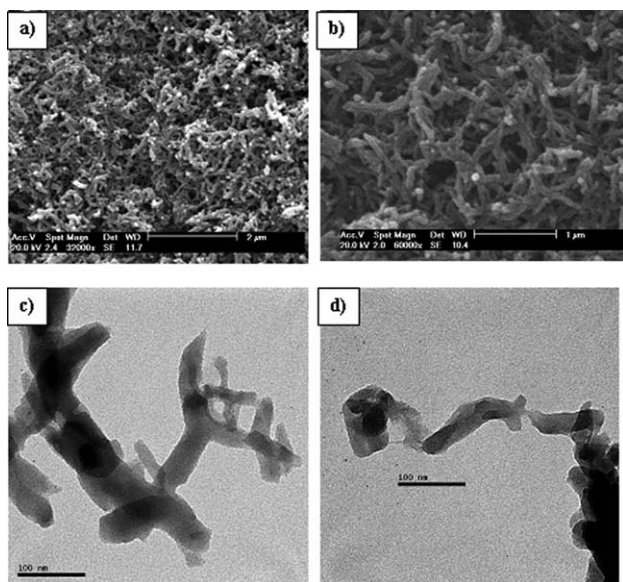


Figure 1. Morphology of PANi-nanofibers: (a and b) SEM images; (c and d) TEM images.

yielding small discs (13 mm in diameter and 1.0 or 2.5 mm thickness). Four probes were connected to the circular sample and the Van der Pauw method was followed.¹⁴ In this method, the current is introduced in a couple probes and the potential difference is measured at the other pair.

The electrical properties of the nanofibers and nanocomposites were also determined with a two-probe Keithley multimeter 2700. Silver paint was coated on the surface of the samples to decrease the contact resistance.

RESULTS AND DISCUSSION

PANi-Nanofiber Preparation and Characterization

PANi-nanofibers were produced by the interfacial polymerization approach in which aniline was dissolved in toluene phase and ammonium peroxydisulfate (APS) dissolved in aqueous chloride acid phase. When the two solutions were slowly put in contact, green PANi was formed first at the interface and then migrated into the aqueous phase, avoiding secondary growth of PANi that would result in the formation of irregularly shaped agglomerates.^{5,15} Figure 1 shows typical SEM and TEM images of the synthesized PANi-nanofibers. Nanofibers characterized by

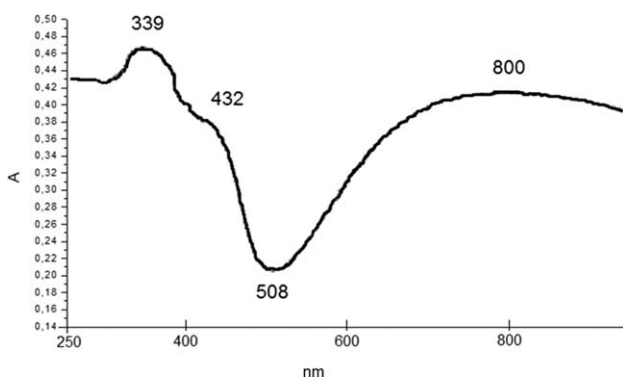


Figure 2. UV-Vis spectrum of PANi-nanofibers.

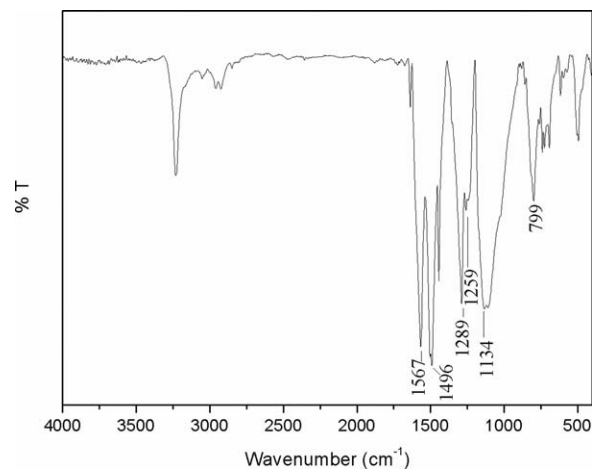


Figure 3. FTIR spectrum of PANi-nanofibers.

high aspect ratio proved to form a largely interconnected network.

The molecular structure of the PANi-nanofibers was evaluated by FTIR and UV-Vis spectroscopies. Three characteristic absorption bands appeared in the UV-Vis spectrum of doped nanofibers corresponding to PANi in its emeraldine salt form (Figure 2). The first absorption band with maximum at 339 nm is associated with the π - π^* electron transition of the benzenoid segments, the second and third absorption bands at 432 and 800 nm are related to the acid-doped state and polaron formation, respectively.¹⁶ The FTIR spectrum of PANi-nanofibers (Figure 3) shows structural characteristics consistent with previous reports^{17,18}: absorption bands in the spectrum are observed at around 1570 and 1500 cm^{-1} (quinoid and benzenoid stretching rings, respectively), in the range of 1290–1250 cm^{-1} (C–N stretching of aromatic secondary amines), 1130–1140 cm^{-1} (C=N stretching) and around 800 cm^{-1} (1,4-substituted phenyl ring stretching).

Figure 4 presents the DSC thermogram of doped PANi-nanofibers. Three endothermic peaks are observed below 100°C, at around 145°C and around 170°C, respectively assigned to loss of H_2O , free (unbound) HCl and some unreacted monomer

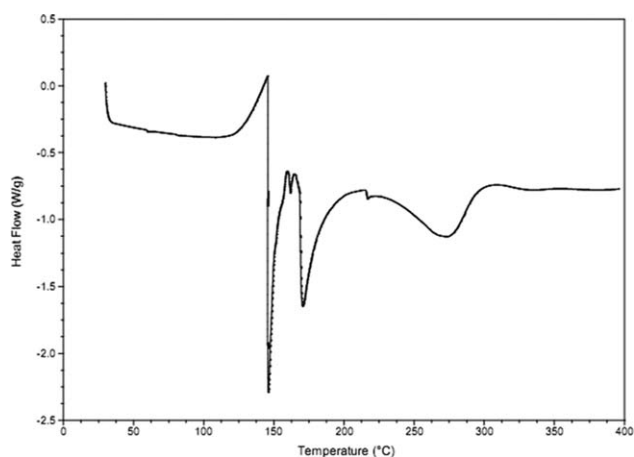


Figure 4. DSC (first heating scan, see experimental) of PANi-nanofibers.

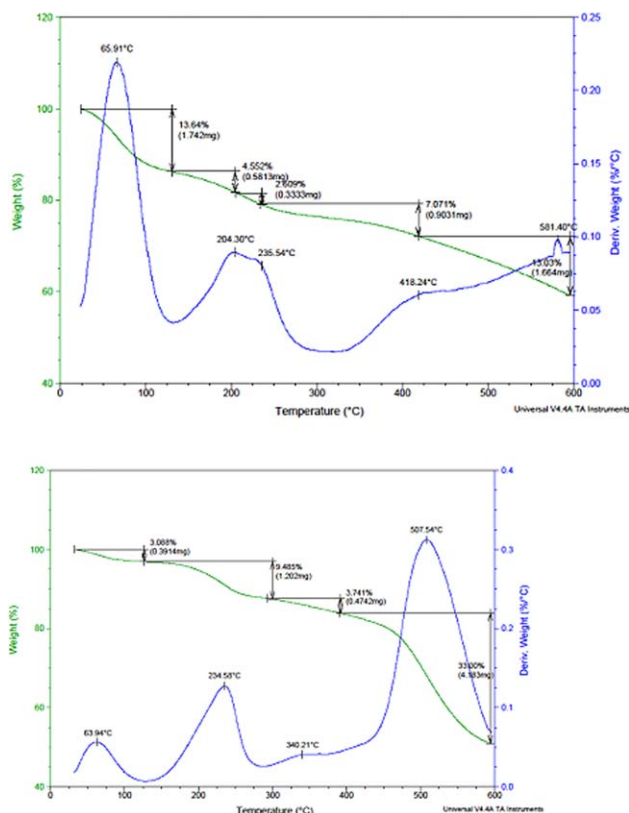


Figure 5. TGA (weight loss curve and deriv. weight) curves of PANi-nanofibers (a) before and (b) after extraction/drying treatment (see text). [Color figure can be viewed in the online issue, which is available at wileyonlinelibrary.com.]

as already reported in the literature.¹⁹ The large peak centered around 270°C may be related to removal of water molecules bonded to polymeric chains, which act as a secondary dopant.^{10–12} The glass transition temperature (T_g) of the PANi-nanofibers is not readily detected. Indeed, the T_g values reported in the literature for PANi vary from 36 to 250°C evidencing its difficulty to be localized.^{12,20–23} The T_g value depends on various parameters such as the processing temperature, heat treatment time, type and concentration of the dopant, content in remaining solvent.¹² To better highlight the T_g value

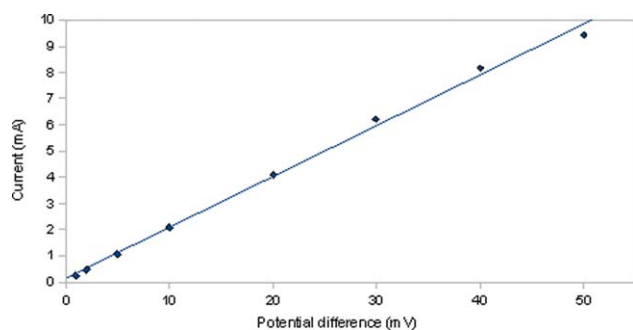


Figure 6. Electrical resistivity measurement of the PANi-nanofibers. A linear regression evidences the ohmic behavior of the produced sample. [Color figure can be viewed in the online issue, which is available at wileyonlinelibrary.com.]

a second heating run was performed (not shown here) but no more thermal event could be observed. Similar results were reported by Ding et al.²⁰ and according to their interpretations this absence of thermal transition indicates a morphological change in PANi during the thermal treatment process, which likely increases the T_g to a value close to the decomposition temperature.²⁰

The TGA curve of the PANi-nanofibers (Figure 5) appears in good agreement with the observations previously achieved by DSC. The first step of weight loss below 100°C is likely due to unbound water,¹¹ the second step of weight loss occurring between 150°C and 300°C may be attributed, respectively, to the unbound HCl (as well as some remaining monomer) and to bound water acting as secondary dopant. The last step of weight loss observed in the range 300–380°C is because of the loss of the primary dopant, that is, HCl.^{24,25} According to the literature the thermal decomposition of PANi with final carbonization of the intermediate compounds is observed over the temperature range of 450–800°C.^{11,25} MAO-based catalytic system is known to be very sensitive to protic contaminants. Therefore, in order to prevent its deactivation, both water and free HCl have to be removed. For that purpose, an additional step of washing and drying of PANi-nanofibers was considered. More specifically, PANi-nanofibers were further washed with water/acetone solution until pH = 4 was reached as above this pH, the conductivity of PANi is known to decrease drastically.²⁶ Then, the samples were intensively dried under vacuum oven at 80°C for ~30 h. Figure 5(b) shows the TGA analyses after this additional treatment of the PANi-nanofibers. The TGA curve clearly highlights the disappearance of both peaks initially present at 50–100°C and 100–200°C attributed to water and free HCl.

The electrical properties of PANi-nanofibers were evaluated through the electrical conductivity (σ) and sheet resistivity (R_s). Figure 6 shows the ohmic characteristic of the sample obtained through the Van der Pauw method. The line slope provided a sample resistance of $0.19 \pm 0.01 \Omega$. Introducing this value in the Van der Pauw formalism one obtains a sheet resistance of $0.96 \pm 0.05 \Omega$. Considering the sample thickness it is possible to obtain its resistivity, $0.24 \pm 0.01 \Omega\text{-cm}$, and conductivity, that is, $4.19 \pm 0.21 \text{ S cm}^{-1}$. Interestingly, the electrical conductivity of the nanofibers obtained in this work appears of high value with respect to other values reported in the literature, especially those obtained using interfacial polymerization process.^{1,5,13,27–29}

After the additional treatment of PANi-nanofibers in order to remove residual impurities, the conductivity value proved to decrease down to $2.2 \times 10^{-2} \text{ S cm}^{-1}$. Actually such a decrease is expected because during the treatment, next to the removal of free HCl, PANi-nanofibers were partially deprotonated as well leading to some reduction of the initially recorded electrical conductivity value obtained via interfacial polymerization methodology.

Preparation and Characterization of PE-Based Nanocomposites Filled with PANi-Nanofibers

The nanocomposites were produced by means of metallocene/MAO-catalyzed *in situ* polymerization of ethylene directly performed in presence of the PANi-nanofibers. From Figure 5(b), it

Table I. Catalytic Activity of the Prepared Nanocomposites and the Relative Content of PANi-Nanofibers in the *In Situ* Produced PE-Based Nanocomposites

Entries	Weight of PANi (g)	Weight of composite (g)	% PANi ^a	Catalytic activity ^b
1	–	4.7730	–	2983
2	0.0024	1.4750	0.2	590
3	0.0245	4.5333	0.5	1813
4	0.0483	2.0074	2.0	1441
5	0.0952	1.7460	5.0	2169
6	0.2401	3.3805	7.0	2113

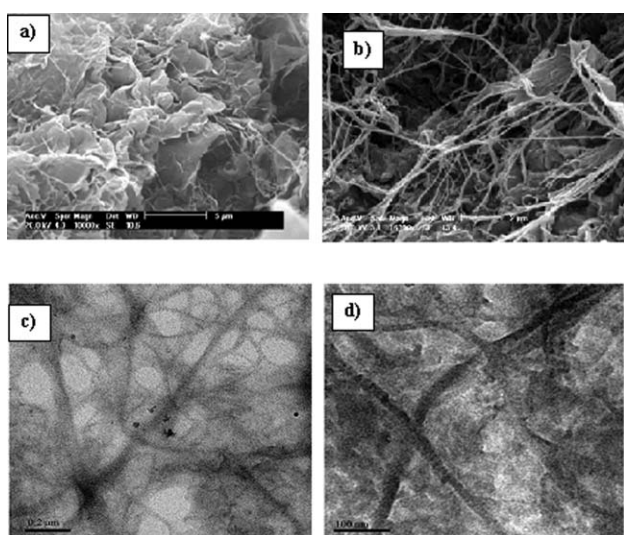
^aPercentage of nanofibers calculated in accordance with nanocomposite yield.

^b(kgPol/molZr.h.bar).

is possible to observe that there is some residual moisture remaining present in the nanofibers, even after drying under vacuum. In order to remove any residual water, PANi-nanofibers were dried under vacuum for more than 2 h and then impregnated with MAO in toluene before polymerization.

Table I shows the catalytic activity determined in function of the starting content in PANi-nanofibers introduced in the polymerization medium (see experimental). It is important to note, that without the treatment of nanofibers to remove free HCl the catalytic activity proved to be very low and in some cases simply nonexistent. After the treatment, HCl remains trapped within the core of the PANi-nanofibers, thus acting as primary dopant, but at the surface it does not show deactivation ability onto the polymerization catalytic system (Table I).

From Table I, it can be observed that even if the catalytic activity is maintained in the presence of the treated PANi-nanofibers, it is reduced with respect to the production of neat polyethylene.

**Figure 7.** SEM images of (a) neat PE and (b) PE/PANI-nanofiber nanocomposites (with 2.0 wt % in PANi); TEM images (c and d) of PE/PANI-nanofiber nanocomposites (with 2.0 wt % in PANi) at two different scales.**Table II.** Melting Temperature (T_m), Enthalpy of Fusion (ΔH), and Degree of Crystallinity of PE (X_c)

Sample codes	ΔH (J/g)	T_m ($^{\circ}\text{C}$)	T_c ($^{\circ}\text{C}$)	X_c (%)
PEPANI 0%	224	133	117	78
PEPANI 0.2%	128	135	118	47
PEPANI 2.0%	141	131	119	52
PEPANI 5.0%	213	133	119	74
PEPANI 7.0%	187	130	118	69

Remarkably, by increasing the relative content in treated nanofibers some increase of catalytic activity is observed (even if the higher recorded value remains below the activity observed for neat PE). A kinetic study of polymerization of ethylene in presence of nanofibers and differential pulse voltammetry of PANi in presence of MAO/catalyst/ethylene are being conducted to understand the interaction of PANi with the catalytic system and will be discussed in a future paper.

SEM and TEM images recorded on the recovered nanocomposites (Figure 7) show that the filler addition changes the morphology of the produced polyethylene. All nanocomposites displayed a structure similar to PANi-nanofibers suggesting that the polymer chains grew around the nanofibers. When

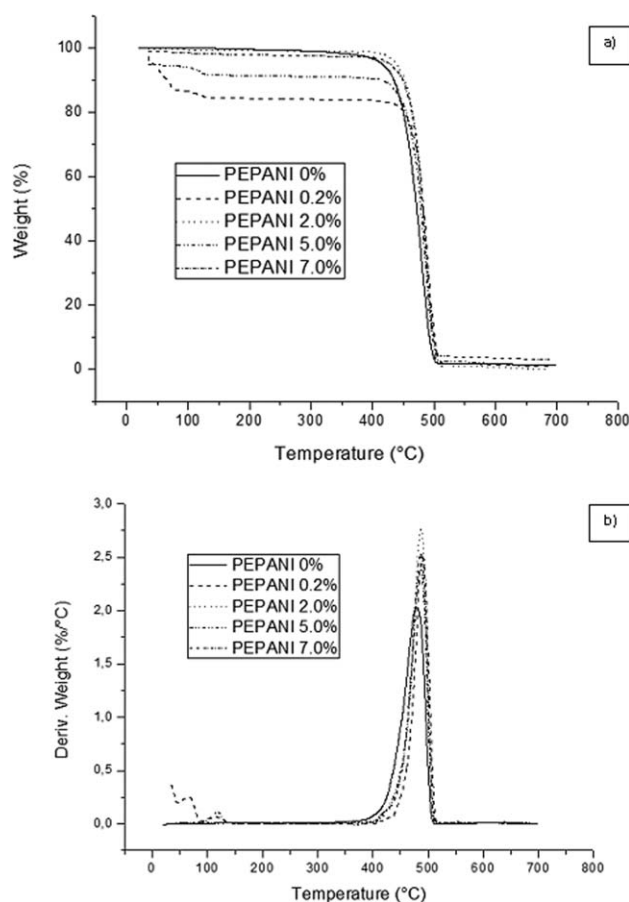
**Figure 8.** TGA curves (and related deriv. weight) of neat PE and related nanocomposites as recorded under nitrogen.

Table III. Temperature of Thermal Degradations (from TGA curves) for Neat PE and Related Nanocomposites

Sample	T_{onset} (°C)	T_{max} (°C)
PEPANI 0%	442	480
PEPANI 0.2%	437	488
PEPANI 2.0%	419	487
PEPANI 5.0%	419	486
PEPANI 7.0%	412	487

compared with the samples obtained by melt blending, *in situ* polymerization is a softer process allowing for preserving the aspect ratio of the filler, dispersing it uniformly in the *in situ* grown polymeric matrix and improving the “filler-polymer” interfacial interaction (actually, mostly via physical adsorption).³⁰ Moreover, a good adhesion between the nanofiber and polymer matrix should result in nanocomposites characterized by improved mechanical properties.³¹

Interestingly enough, the DSC analysis shows that the addition of PAni-nanofibers only slightly changes the melting temperature of the resulting high density PE-based nanocomposites with melting temperature values ranging between 127 and 133°C (Table II). As far as the degree of crystallinity of the polyolefinic matrix is concerned, a decrease is observed in presence of PAni-nanofibers. However, by increasing the nanofiber content, the crystallinity difference between neat HDPE and nanocomposites tends to be reduced. More studies (under current investigation) are necessary to understand such an effect but at this stage this is far beyond the scope of this contribution.

Figure 8 shows TGA thermograms of neat PE and the nanocomposites as recorded under N_2 . The maximum of degradation temperature of the nanocomposites is around 480°C, no significant change is observed when compared with neat PE. However, the onset degradation temperature is found to be slightly lower than in the case of neat PE (Table III). This result is related to the early degradation of PAni.

Concerning the ability of PAni-nanofibers to bring electrical properties to PE-based polymers, several studies are reported in the literature. Most of them focus on the melt blending approach of PAni-nanoparticles within PE matrix. For instance, Su et al. prepared by melt processing ternary composites of PAni nanofibers doped with dodecylbenzenesulfonic acid (PAni-DBSA) and low density polyethylene (LDPE) and ethylene-acrylic acid copolymer (EAA) as compatibilizer. Their results showed that percolation threshold occurs at about 4% of

Table IV. Volume Resistivity of PE/PAni-Nanofiber Nanocomposites Prepared by *In Situ* Polymerization

Composition	Volume resistivity (Ω cm)
PEPANI 0%	10^{15}
PEPANI 0.5%	10^8
PEPANI 1.0%	10^4

PAni-DBSA and to reach a conductivity of $8 \times 10^{-5} \text{ S cm}^{-1}$, 20 wt % of PAni nanofibers were required for PAni/LDPE/EAA (20/64/16) composites.²⁷ Löfgren et al.³² investigated the use of functionalized polyethylene to compatibilize PE with PAni nanofibers. They prepared blends by melt mixing with PAni amounts ranging from 2 to 18 wt % and they found 15 wt % was needed to reach electrical conductivity around $3 \times 10^{-5} \text{ S cm}^{-1}$. Zhang et al. dispersed PAni-DBSA in the matrix LDPE. Their results showed that the conductivity of the composites was $10^{-6} \text{ S cm}^{-1}$ and $10^{-3} \text{ S cm}^{-1}$, respectively, when the weight fraction of PAni filler was 10 wt % and 25 wt %.³³ To summarize the literature results, it appears that via direct melt blending approach, the amount of PAni-nanofibers required to achieve PE materials with dissipative electrical conductivity is quite high. In Table IV, volume electrical resistivity of the PE-based nanocomposites as prepared following our procedure by *in situ* polymerization are gathered.

It appears that after PAni-nanofibers underwent the treatment to remove water and free HCl, *in situ* polymerization of ethylene can successfully take place leading to composites, which exhibit promising electrical properties, reaching a volume resistivity of $10^4 \Omega \cdot \text{cm}$. Moreover, *in situ* polymerization allows a better controlled process when compared with direct melt blending compounding and a better tuning of morphology and improved electrical properties of PAni/PE composites can thus be expected. These points will be discussed in a forthcoming paper.

CONCLUSIONS

PAni-nanofibers were successfully synthesized and characterized by SEM, TEM, FTIR, UV-Visible, DSC, and TGA. The measurement of the electric properties indicates an ohmic behavior of PAni-nanofibers stressing their potentiality to be used as conductive nanofillers. PAni-filled polyethylene nanocomposites were successfully prepared by *in situ* polymerization of ethylene directly catalyzed in the presence of PAni-nanofibers. It was necessary to adapt and modify the process of PAni-nanofibers manufacture by adding a supplementary step to remove the unbounded water as well as the excess of HCl dopant, which can deactivate the MAO-based catalytic system and prevent ethylene from polymerizing. The resulting materials exhibited high potential as it appeared that PAni-nanofibers affect significantly the PE crystallinity while preserving the thermal stability of PE matrix. Preliminary measurements of electric properties show PAni-nanofibers are able to bring electro-conductive properties to the *in situ* polymerized PAni/PE nanocomposites. All these results are very promising in the search for new materials for engineering applications requiring electrical conductivity.

ACKNOWLEDGMENTS

The authors thank CAPES, CNPq, and FAPERGS for financial support. Materia Nova authors thank the European Community for financial support framing the 7th Framework Program research project “HARCANA” (Grant Agreement No: NMP3-LA-2008-213277). MATERIA NOVA and CIRMAP thank the “Belgian Federal Government Office Policy of Science (SSTC)” for general support in

framing the PAI-6/27 and “Region Wallonne” in framing the “Programme d’Excellence: OPTI²MAT.” The Authors also thank the Belgian Federal Science Policy Office for research fellowship.

REFERENCES

1. Bhadra, S.; Khastgir, D. N. K.; Singhaa, J. H. *Progr. Polym. Sci.* **2009**, *34*, 8, 783.
2. Kaner R. B.; Huang, J. *Angew Chem. Int. Ed.* **2004**, *43*, 5817.
3. Zhang, D.; Wang, Y. *Mater. Sci Eng. B.* **2006**, *134*, 9.
4. Annala, M.; Löfgren, M. B. *Macromol. Mater. Eng.* **2006**, *291*, 848.
5. Huang, J.; Kaner, R. B. *J. Am. Chem. Soc.* **2004**, *126* 851.
6. Tsocheva, D.; Terlemezyan, L. *J. Thermal Anal. Calorimetry* **2005**, *81*, 3.
7. Alexandre, M.; Pluta, M.; Dubois, P.; Jérôme, R. *Macromol. Chem. Phys.* **2001**, *202*, 2239.
8. Fim, F de C.; Guterres, J.; Basso, N. R. S.; Galland, G. B. *J Polym Sci Part A: Polym Chem* **2010**, *48*, 692.
9. Scheirs, J.; Kamisky, W. *Metalocene-based Polyolefins: Preparation, Properties, and Technology*; Wiley and Sons: Chichester, **2000**.
10. Matveeva, E. S.; Calleja, R. D.; Parkhutik, V. P. *Syn. Metals* **1995**, *72*, 105.
11. Sinha, S.; Bhadra, S.; Khastgir, D. *J. Appl. Polym. Sci.* **2009**, *112*, 3135.
12. Bhadra, S.; Khastgir, D. *Syn. Metals* **2009**, *159*, 1141.
13. King, R. C. Y.; Roussel, F. *Syn. Metals* **2005**, *153*, 337.
14. Pauw, L. J. *Philips Res. Reports* **1958**, *13*, 1.
15. Huang, J.; Virji, S.; Weiller, B. H.; Kaner, R. B. *J. Am. Chem. Soc.* **2003**, *125*, 314.
16. Huang, Y. F.; Lin, C. W. *Syn. Metals* **2009**, *159*, 1824.
17. Ge, C.; Yang, X.; Li, C.; Hou, B. *J. Appl. Polym. Sci.* **2011**, *123*, 627.
18. Jang, J.; Bae, J.; Lee, K. *Polymer* **2005**, *46*, 3677.
19. Ansari, R.; Keivani, M. B. E. *J. Chem.* **2006**, *3*, 202.
20. Ding, L.; Wang, X.; Gregory, R. V. *Syn. Metals* **1999**, *104*, 73.
21. Pham, Q. M.; Kim, J. S.; Kim, S. *Syn. Metals* **2010**, *160*, 394.
22. Abell, L.; Pomfret, S. J.; Adams, P. N.; Monkman, A. P. *Synth. Metals* **1997**, *84*, 127.
23. Emirkhaniana, R.; Salvia, M.; Ferreira, J.; Jaffrezic, N.; Chazeau, L.; Mazzoldi, A. *Mater. Sci. Eng. C* **2006**, *26*, 227.
24. Bhadra, S.; Khastgir, D. *Polym. Degrad. Stab.* **2007**, *92*, 1824.
25. Bhadra, S.; Khastgir, D. *Polym. Degrad. Stab.* **2008**, *93*, 1094.
26. Diarmid, A. G.; Chiang, J. C.; Richter, A. F.; Epstein, A. J. *Synth. Metals* **1987**, *18*, 285.
27. Su, S.; Wang, G.; Huang, F.; Li, X. *Polym. Comp.* **2008**, *1177*.
28. Xing, S.; Zhao, C.; Jing, S.; Wang, Z. *Polymer* **2006**, *47*, 2305.
29. Sinha, S.; Bhadra, S.; Khastgir, D. *Appl. Polym. Sci.* **2009**, *112*, 3135.
30. Al-Saleh, M. H.; Sundararaj, U. *Carbon* **2009**, *47*, 2.
31. Chipara, M.; Hui, D.; Notingher, P. V.; Chipara, M. D.; Lau, K. T.; Sankar, J.; Panaitescu, D. *Composites: Part B* **2003**, *34*, 637.
32. Löfgren, B.; Annala, M. *Macromol. Mater. Eng.* **2006**, *291*, 848.
33. Zhang, Q. H.; Wang, X. H.; Chen, D. J.; Jing, X. B. *Syn. Metals* **2003**, *135*, 481.